Polymer 51 (2010) 5921–5928

Contents lists available at ScienceDirect

Polymer

journal homepage: www.elsevier.com/locate/polymer

In-situ synthesis and characterization of electrically conductive polypyrrole/graphene nanocomposites

Saswata Bose [a], Tapas Kuila [a], Md. Elias Uddin [a], Nam Hoon Kim [b], Alan K.T. Lau [a,c], Joong Hee Lee [a,b,*]

[a] WCU Program, Department of BIN Fusion Technology, Chonbuk National University, Jeonju, Jeonbuk 561-756, Republic of Korea
[b] Department of Hydrogen and Fuel Cell Engineering, Chonbuk National University, Jeonju, Jeonbuk 561-756, Republic of Korea
[c] University of Southern Queensland, Toowoomba, Australia

ARTICLE INFO

Article history:
Received 14 August 2010
Received in revised form
7 October 2010
Accepted 10 October 2010
Available online 16 October 2010

Keywords:
Graphene nanosheets
Nanocomposites
Polypyrrole

ABSTRACT

Polypyrrole (PPy)/graphene (GR) nanocomposites were successfully prepared via in-situ polymerization of graphite oxide (GO) and pyrrole monomer followed by chemical reduction using hydrazine monohydrate. The large surface area and high aspect ratio of the in-situ generated graphene played an important role in justifying the noticeable improvements in electrical conductivity of the prepared composites via chemical reduction. X-ray photoelectron spectroscopy (XPS) analysis revealed the removal of oxygen functionality from the GO surface after reduction and the bonding structure of the reduced composites were further determined from FTIR and Raman spectroscopic analysis. For PPy/GR composite, intensity ratio between D band and G band was high (~ 1.17), indicating an increased number of c-sp^2 domains that were formed during the reduction process. A reasonable improvement in thermal stability of the reduced composite was also observed. Transmission electron microscopy (TEM) observations indicated the dispersion of the graphene nanosheets within the PPy matrix.

1. Introduction

Graphene nanosheets, monolayers of carbon atoms, have drawn the attention of researchers owing to their astonishing electronic, thermal, and mechanical properties [1–7]. Ballistic movement of electrons through the graphene structure causes improvement in electrical properties [8,9]. Owing to a high aspect ratio, outstanding electrical conductivity and cost efficiency, graphene can act as an effective conductive filler in polymer as compared to carbon nanotubes [3,10,11]. However effectiveness of graphene as nanofiller can be exploited via the incorporation of graphene sheets into composite materials. Hence, investigation of graphene-based polymer composites is an issue of rapidly growing interest to the researchers over the world. Graphene can be synthesized very easily by the chemical reduction of graphite oxide (GO). GO can be prepared from natural graphite by the Hummers method from natural graphite [12] and it is hydrophilic in nature as it contains several oxygen functionalities, such as hydroxyl, epoxy, carbonyl and carboxyl [13–15]. Till date several researches have been carried out based on graphene/polymer composites using graphene as nanofiller [16–18]. Stankovich et al. [3] developed polystyrene–graphene composites by adopting solution–phase mixing of surface modified graphite oxide sheets with polystyrene followed by their chemical reduction. Chen et al. [19] prepared GNS/polymer composites by ultrasonication of expanded graphite (EG) in a liquid medium, followed by in-situ polymerization. PANI/Graphene composites were prepared by Zhang et al. [20] by in-situ polymerization procedure.

Conducting polymers are well-known for their easy processability and outstanding electrical properties. Among these materials, polypyrrole (PPy) has been considered as one of the most promising electrode materials because of its low cost, easy synthesis and relatively high conductivity [21,22]. In order to exploit the electrical performance of PPy, nanometer-sized fillers with conductive path structure and high surface area should be considered. Graphene (GR) can be considered as nanosized-filler for PPy due to their high surface area and excellent conductivity [3,23].

Until recently, efforts have been made to improve the electrical conductivity of PPy using GO [24]. However, in the current study, preparation of PPy/GR composites via in-situ polymerization technique involving pyrrole monomer and GO, followed by chemical reduction using hydrazine monohydrate has been demonstrated. Accordingly, this study is aimed at achieving a dispersion of

* Corresponding author. WCU Program, Department of BIN Fusion Technology, Chonbuk National University, Jeonju, Jeonbuk 561-756, Republic of Korea. Tel.: +82 63 270 2342; fax: +82 63 270 2341.
E-mail address: jhl@chonbuk.ac.kr (J.H. Lee).

0032-3861/$ – see front matter © 2010 Elsevier Ltd. All rights reserved.
doi:10.1016/j.polymer.2010.10.014

GR sheets within the polymer matrix, yielding reasonable electrical and thermal properties.

2. Experimentation

2.1. Materials used

Natural flake graphite was purchased from Sigma Aldrich. Sulfuric acid, hydrochloric acid, ethanol and Hydrogen peroxide were purchased from Samchun Pure Chemical Co. Ltd., Korea. Potassium permanganate, as oxidizing agent was purchased from Junsei Chemical Co. Ltd., Japan and Hydrazine monohydrate, as reducing agent was purchased from TCI, Japan. Pyrrole monomer, having molar mass of 67 g/mol and density of 0.97 g/cc, was purchased from Sigma Aldrich.

2.2. Preparation and reduction of graphite oxide (GO)

GO was prepared by following modified Hummers method. In the typical procedure, graphite (2.0 g) was mixed with 46 mL of H_2SO_4 (95%) and the mixture was stirred for 30 min within an ice bath. Potassium permanganate (6.0 g) was added very slowly in the suspension with vigorous stirring while maintaining a reaction temperature of 20 °C. Then the ice bath was removed, and the reaction mixture was stirred overnight at 35 °C. In the next step water was added to the pasty solution with constant agitation. Thereupon, the colour of the solution changed to yellowish brown. After 2 h of vigorous stirring, 50 mL of 30% H_2O_2 was added and immediately the colour turned golden yellow. The mixture was washed several times with 5% HCl and then deionized (DI) water until the solution became acid free. Then the reaction mixture was filtered and dried under vacuum at 65 °C. The GO was obtained as a gray powder. In order to carry out the reduction, 0.1 g of GO was dispersed in 50 mL of DI water. Then 1 mL of hydrazine monohydrate was added to the mixture and heated at 95 °C for 12 h. After the completion of the reaction, the reduced graphite oxide was collected by filtration as a black powder. The product thus obtained was washed with DI water several times to remove excess hydrazine, and the final product was dried in a vacuum oven at 75 °C for 24 h.

2.3. Synthesis of polypyrrole (PPy)

Firstly, the pyrrole monomer was purified by column chromatography technique in order to remove the impurities, followed by distillation under vacuum. The distilled pyrrole (0.2 M) was then dissolved in 50 mL mixture of water and ethanol (1:1) mixture. Ferric chloride (0.1 M) in 50 mL of water was added to the solution of pyrrole. Immediately the polymerization was initiated and the reaction was allowed to continue for 24 h at room temperature with continuous stirring. The black polymer thus obtained was collected via filtration, washed several times with water and ethanol mixture in order to remove excess ferric chloride. The as-synthesized polymer was then dried under vacuum at 60 °C for 24 h. Finally, the polypyrrole (0.63 g) was collected with a yield of 45.6%.

2.4. Synthesis of PPy/GO and PPy/GR composites

The PPy/GO composites were prepared by in-situ polymerization involving pyrrole and graphite oxide. The weight feed ratio of pyrrole to graphite oxide was varied as 95:5, and 88:12, and 80:20 and the resulting composites were designated as PPyGO1, PPyGO2 and PPyGO3. Firstly, GO was dispersed in 50 mL of water by ultrasonication for 30 min. Conversely, pyrrole (0.2 M) was dissolved in 30 mL of 1:1 water and ethanol mixture. The resultant solution was added to the dispersion of GO and ultrasonication was continued for another 30 min. After that ferric chloride solution (0.1 M ferric chloride in 20 mL of water) was added drop wise to the mixture of pyrrole and GO, the polymerization started immediately and the reaction was allowed to continue for 24 h under vigorous stirring. The composite thus obtained was washed several times with mixture of water and ethanol. Finally the composites were dried under vacuum at 60 °C for 24 h.

PPy/GR composites were prepared via the same procedure, adapted for the preparation of GR from GO. 0.1 g of PPy/GO composites (PPyGO1, PPyGO2 and PPyGO3) was heated in 1 mL of hydrazine monohydrate at 95 °C for 12 h. After the completion of reaction, the reduced composites were collected by filtration, followed by several washings with DI water and ethanol to remove excess hydrazine. The final product was dried in a vacuum oven at 75 °C for 24 h and designated as PPyGR1, PPyGR2 and PPyGR3 respectively. Proposed mechanism of synthesis of PPy/GO and PPY/GR composites from GO is shown in Fig. 1.

3. Characterization

3.1. Gel permeation chromatography (GPC)

The molecular weight of polypyrrole was determined by gel permeation chromatography (TOSOH ECOSEC, HLC-8320) using TOSOH, TSK_{gel} (Super AWM-H) column. The calibrations were done by Polystyrene standards (Tosoh, TSK) ranging from 2500 to 1110,000 g/mol.

3.2. Fourier transformed infrared spectroscopy (FTIR)

FTIR study of pure PPy and the composites were carried out using a Nicolet 6700 spectrometer (Thermoscientific, USA) at room temperature over a frequency range of 4000–500 cm^{-1}.

3.3. X-ray diffraction (XRD) study

The crystallographic structures of the materials were determined via XRD study. The XRD analysis was performed using a D/Max 2500V/PC diffractometer (Rigaku Corporation, Japan) with Cu–Kα targets ($\lambda = 0.154$ nm) at a scanning rate of 0.020 2θ/s, chart speed of 10 mm/2θ, and operated at a voltage of 40 kV and current of 100 mA.

3.4. X-ray photoelectron spectroscopy (XPS)

The chemical nature of the pure graphene and its in-situ composites with polypyrrole was analyzed by XPS (AXIS-NOVA, Kratos Analytical Ltd, UK).

3.5. Raman spectroscopy

Raman spectra were recorded in the range of 700–2100 cm^{-1} in a Nanofinder 30 confocal Raman Microscope (Tokyo instruments Co., Japan) using a He–Ne laser beam having a wave length of 488 nm with a CCD detector.

3.6. Electrical conductivity measurements

Measurements of electrical conductivities of the samples were performed using Keithley 2000 (Keithley Instruments Inc., USA) apparatus. The resistivity of the pressed samples was measured in a four-point probe unit using the following equation:

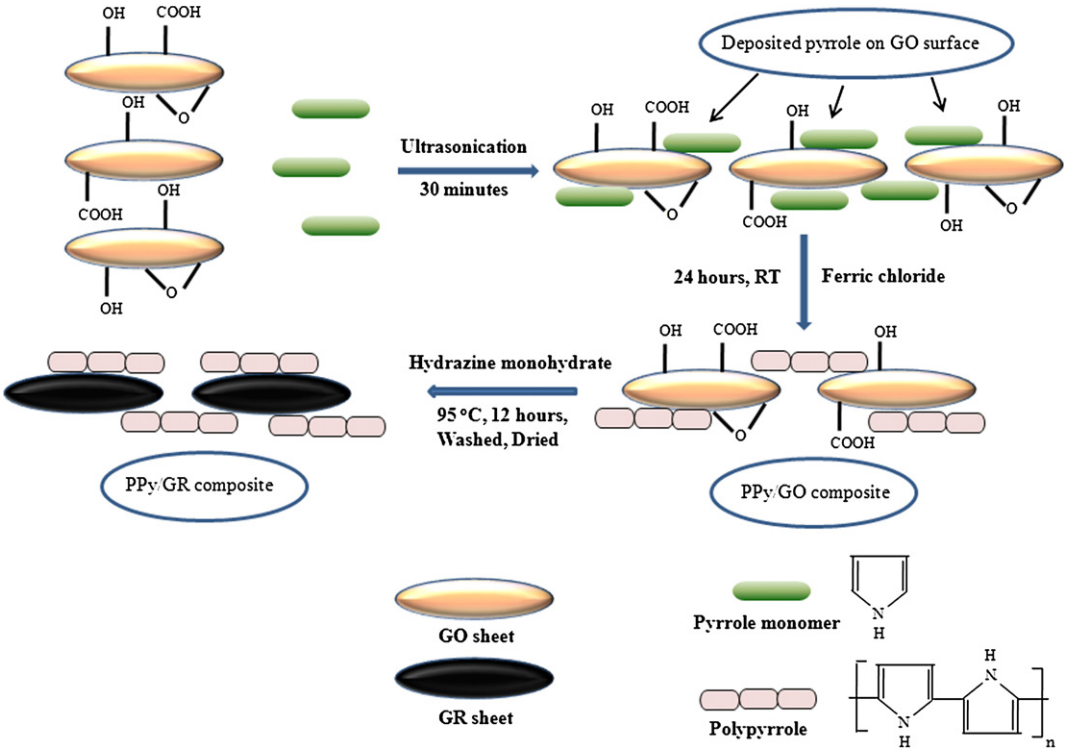

Fig. 1. Proposed mechanism for PPy/GR synthesis.

$$\text{Resistivity}(\rho,\ \text{ohm}-\text{cm}) = \pi t/\ln 2(V/I) = 4.53 \times t \times (\text{resistance})$$

$$\text{Conductivity}(\sigma,\ \text{S/cm}) = 1/\rho$$

Where, t is the thickness of the sample, V is the measured voltage and I is the source current.

3.7. Thermogravimetric analysis (TGA)

Thermogravimetric analysis was conducted under nitrogen atmosphere using Q50 TGA (TA instruments, USA) in the temperature range of 40–700 °C, with a heating rate of 5 °C/minute.

3.8. Field emission scanning electron microscopy (FESEM)

All FESEM measurements were carried out in a JSM-6701F (JEOL, Japan). The powder samples were placed on an aluminum holder and then coated with a thin layer of gold.

3.9. Transmission electron microscopy (TEM)

All TEM measurements were carried out on an H-7650 (Hitachi, Japan) microscope at 120 kV. The TEM samples were prepared by dispersing a small amount of powder sample in ethanol by ultrasonication. A single drop of the suspension was then dropped onto the carbon-coated 300 mesh copper grids for measurements.

4. Results and discussion

4.1. Gel permeation chromatography (GPC)

In a typical experiment, 0.01 g of polymer was dissolved in 10 mL of *N,N*-dimethyl formamide (DMF) followed by filtration using Teflon filter paper. DMF was used as a mobile phase in the experiment. From the experiment it has been observed that the weight average molecular weight (M_w) and the number average molecular weight (M_n) of the polymer were 356,797 and 240,561 respectively with a polydispersity index of 1.48.

4.2. FTIR analysis

FTIR analysis of pure PPy, GO, PPy/GO, and PPy/GR composites are represented in Fig. 2. Peaks at 1548, 1448, and 3451 cm^{-1} are associated with the C–C, C–N, and N–H stretching vibration in the polypyrrole ring. The peaks at 2926 and 2853 cm^{-1} are designated

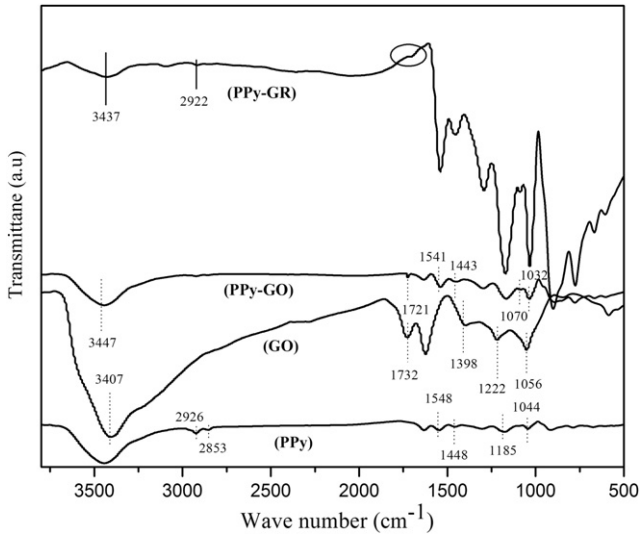

Fig. 2. FTIR spectroscopic analysis of pure PPy, GO, PPy/GO, and PPy/GR composites.

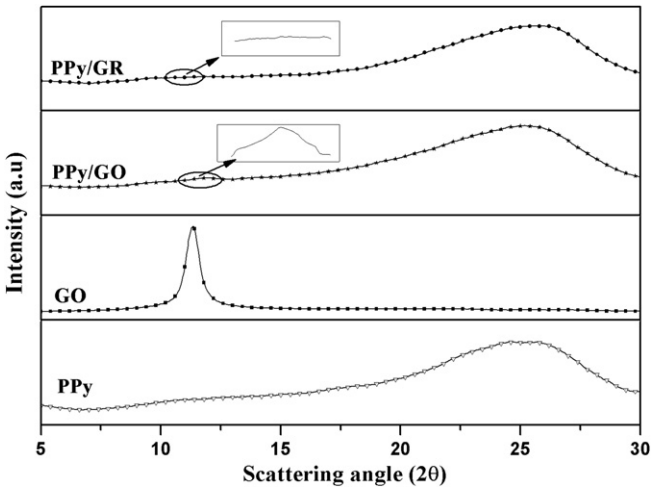

Fig. 3. XRD study of pure PPy, GO, PPy/GO, and PPy/GR composites.

as the asymmetric stretching and symmetric vibrations of CH_2 [22]. The broad peak at 3407 cm^{-1} and a peak at 1732 cm^{-1} in the FTIR spectrum of GO could be assigned to O—H stretching vibration and the carbonyl (C═O) stretching respectively. Two other peaks, one at 1398 cm^{-1} and other at 1222 cm^{-1} represent the O—H deformation and C—OH stretching vibration [25]. Evidence of the epoxide group in the GO layers is confirmed from the peak near 1056 cm^{-1}, representing C—O stretching vibrations. However, for PPy/GO composites the peak due to the COOH group has been downshifted to 1721 cm^{-1} which is probably due to the π–π interaction between the GO layers and aromatic polypyrrole rings [26]. The presence of polypyrrole in the PPy/GO composite is confirmed by the appearance of characteristic peaks of polypyrrole at 1542 and 1443 cm^{-1}. However from the FTIR spectra of PPy/GO composites it has also been observed that the peak at 1044 cm^{-1}, C—H in-plane vibration of polypyrrole ring, shifted to 1032 cm^{-1} and also the peak at 1056 cm^{-1} which is due to epoxy group as mentioned earlier, shifted to 1070 cm^{-1}. The shifting of the peaks as mentioned clearly reveals the change in chemical environment during the formation of in-situ composites involving PPy and GO. The interesting observation is that upon reduction of the PPy/GO composites, the characteristic peak of COOH group of GO at 1720 cm^{-1} is weakened.

4.3. XRD study

The structure of the composites was investigated by X-ray diffraction (XRD) measurements. The XRD patterns of pure PPy, GO, PPy/GO and PPy/GR are shown in Fig. 3. Pure PPy exhibits a broad band at $2\theta = 25.1^\circ$ ($d = 0.35$ nm). A peak at $2\theta = 11.38^\circ$ ($d = 0.78$ nm), appeared in the XRD pattern of GO, corresponds to (001) reflection peak. The value of interlayer spacing depends upon number of water layers in the gallery space of GO [27]. The oxygen functionality on the surface of the GO also played a part in determining the interlayer spacing. For the PPy/GO composite, the peak at 11.38° has shifted to 11.7° ($d = 0.75$ nm) with significant decrease in peak intensity along with a broad band at 25.2°. Decrement in

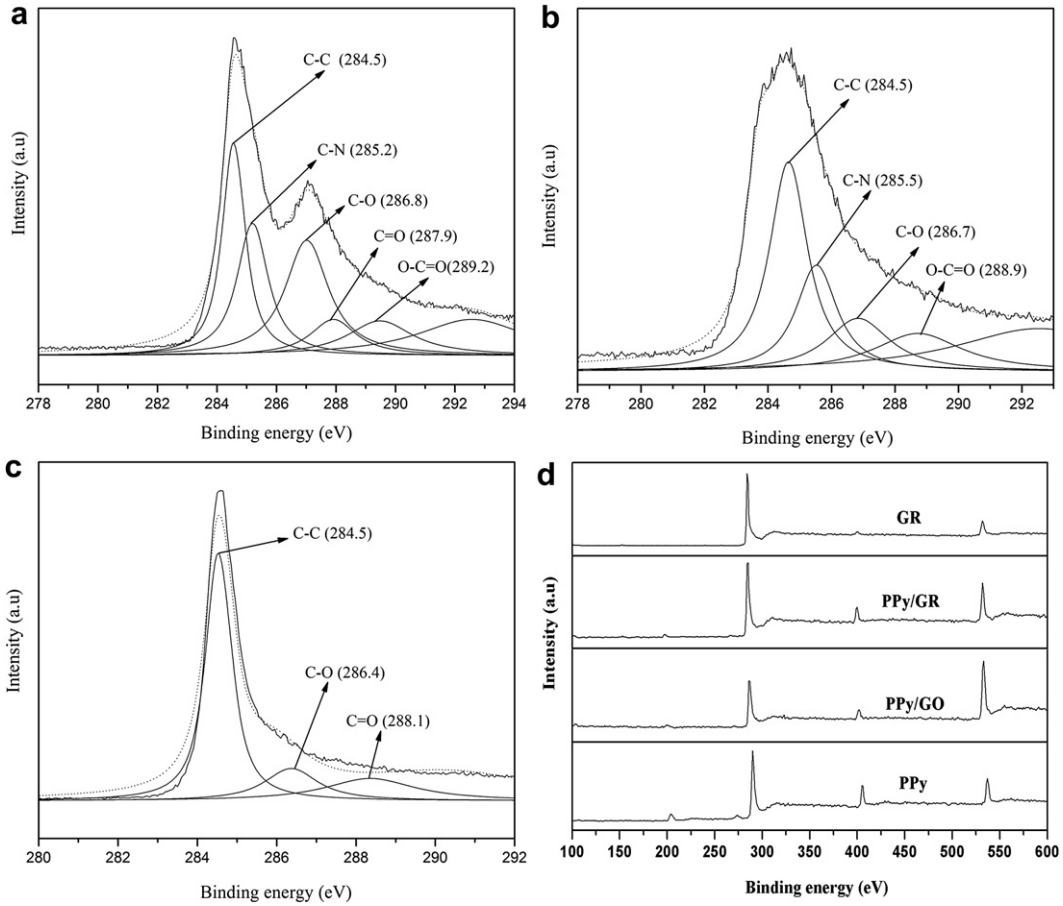

Fig. 4. (a–d): De-convoluted C1s XPS spectra of PPy/GO (a); PPy/GR (b); pure GR (c); wide region XPS study of pure PPy, GR, PPy/GO, and PPy/GR composites (d).

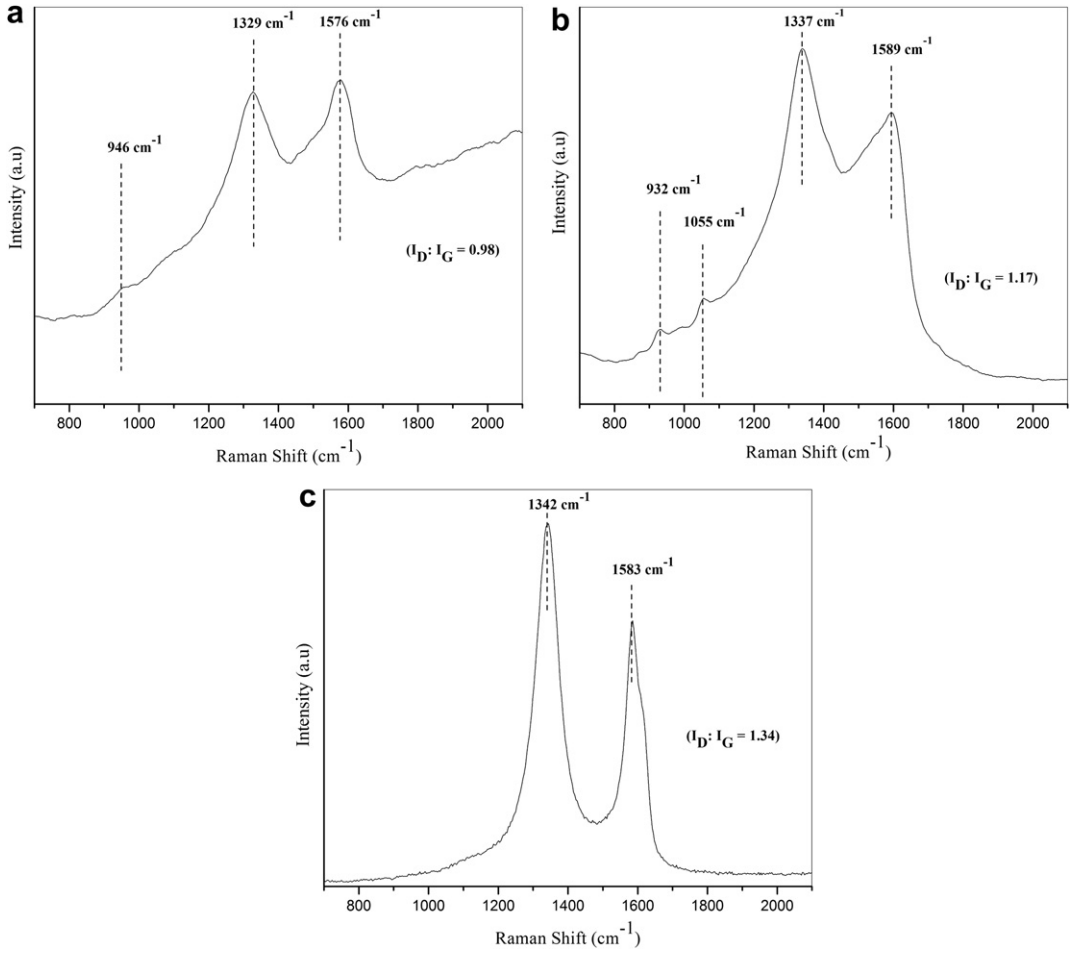

Fig. 5. (a–c): Raman spectra of PPy/GO composite (a); PPy/GR composite (b); pure GR (c).

the peak intensity may perhaps due to exfoliation of GO layers upon ultrasonication. Appearance of peak at $2\theta = 11.7^{\circ}$ (for GO) and $2\theta = 25.2^{\circ}$ (for polypyrrole) in the XRD pattern of the PPy/GO composites corroborated the successful development of the composite. However, it is evident from the XRD pattern of the PPy/GR composite that the peak at 11.38° (characteristic peak of GO) has been disappeared completely suggesting the reduction of the GO to GR.

4.4. XPS analysis

The C1s XPS spectrum of PPy/GO, PPy/GR and pure graphene are depicted in Fig. 4(a–c). Wide region spectroscopy of pure PPy, GR, and the nanocomposites is also shown in Fig. 4d. The deconvoluted C1s spectra of the PPy/GO composites (Fig. 4a) exhibit five Lorentzian peaks with different binding energies. The C1s spectra of non oxygenated carbon, i.e., the graphitic carbon ('C–C') appear at 284.5 eV. The intense peak at 286.8 eV justifies the

Table 1
Conductivity measurements.

Sample	Thickness (d, cm)	Resistance (Ohm)	Resistivity (ρ, ohm-cm)	Conductivity (σ, S/cm)
PPy	0.04	28.000	5.070	0.190
PPy/GO1	0.04	10.661	1.930	0.510
PPy/GO2	0.04	3.910	0.708	1.410
PPy/GO3	0.04	3.157	0.608	1.640
PPy/GR1	0.04	1.876	0.340	2.940
PPy/GR2	0.04	1.192	0.216	4.620
PPy/GR3	0.04	0.699	0.126	7.930
GR	0.04	0.120	0.021	47.600

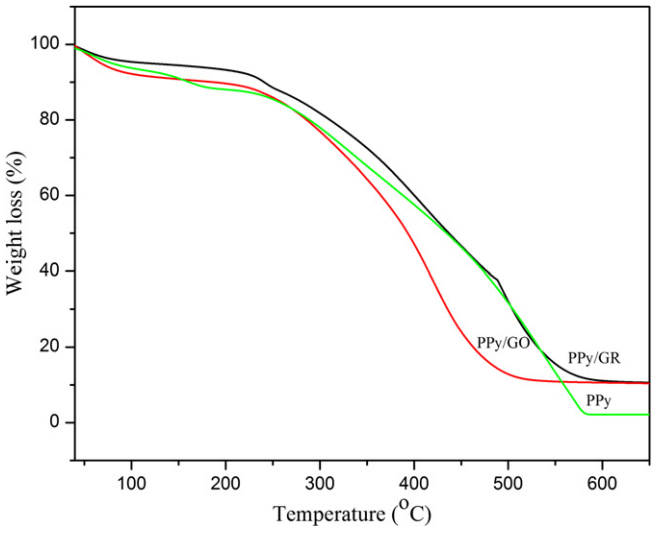

Fig. 6. TGA of pure PPy, GR, PPy/GO, and PPy/GR composites.

Table 2
Thermogravimetric analysis.

Sample	% Of weight loss at 100 °C	% Of weight loss at 200 °C	% Of weight loss at 250 °C	% Of weight loss at 350 °C	% Of weight loss at 450 °C	Retention of % of weight at 650 °C
PPy	6.1	11.6	14.1	31.4	52.7	2.3
PPy/GO	7.9	10.5	14.4	36.2	76.1	10.5
PPy/GR	4.0	6.1	11.1	26.9	52.7	11.2

presence of C–O group. The peaks observed at 287.8, 289.2 and 285.2 eV suggesting the presence of C=O, O–C=O, and C–N group respectively [28,29]. However, substantial reduction in peak intensity of the oxygen functionalities have been observed in the C1s de-convoluted spectra of PPy/GR composites (Fig. 4b) and also the 'C=O' functionality has removed completely, corroborating that lessening of the oxygen functionality upon reduction [29]. XPS spectrum of pure graphene (Fig. 4c) also demonstrates three lorentzian peaks with different binding energies. The peaks observed at 284.5, 286.4 and 288.1 eV justify the presence of C–C, C–O, and C=O group with substantial reduction of peak intensity. The shifting of the peaks in PPy/GR composite as compared to pure graphene indicating the probable interaction between PPy and GR. From careful inspection of wide region spectroscopy (Fig. 4d) and elemental analysis of PPy/GO and PPy/GR composites from XPS study, it could be observed that for PPy/GO composites, the C/O ratio was 2.1 and the same for PPy/GR is 9.9. The percentage of 'O' from GO in PPy/GO composite is 27.76 and the percentage of 'O' from GR in PPy/GR composite is 8.54, indicating that most of oxygen functionality has been successfully removed after reduction. In addition to that percentage of N in the PPy/GO composite is 8.69 and the same in PPy/GR composite is 5.48 corroborating the presence of polypyrrole in the concerned composites.

4.5. Raman spectroscopy

The Raman spectra of PPy/GO, PPy/GR, and pure graphene are shown in Fig. 5(a–c). In the case of the PPy/GO composite, the characteristic D band appeared at 1329 cm^{-1} and the G band at 1576 cm^{-1} (Fig. 5a). The G band represented the first-order scattering of the E_{2g} vibrational mode while the D band has been attributed to the reduction in size of the in-plane C sp^2 atoms [28,30,31]. However, the D and G bands had shifted to 1337 cm^{-1} and 1589 cm^{-1} for the PPy/GR composites (Fig. 5b), while in case of pure graphene the D band appeared at 1342 cm^{-1} and the G band at 1583 cm^{-1} (Fig. 5c). The intensity ratio (I_D:I_G) was 0.98, 1.17, and 1.34 for PPy/GO, PPy/GR and pure graphene respectively. The increment in intensity in chemically reduced composite (PPy/GR), as compared to that of PPy/GO composite may be attributed to the following reasons:

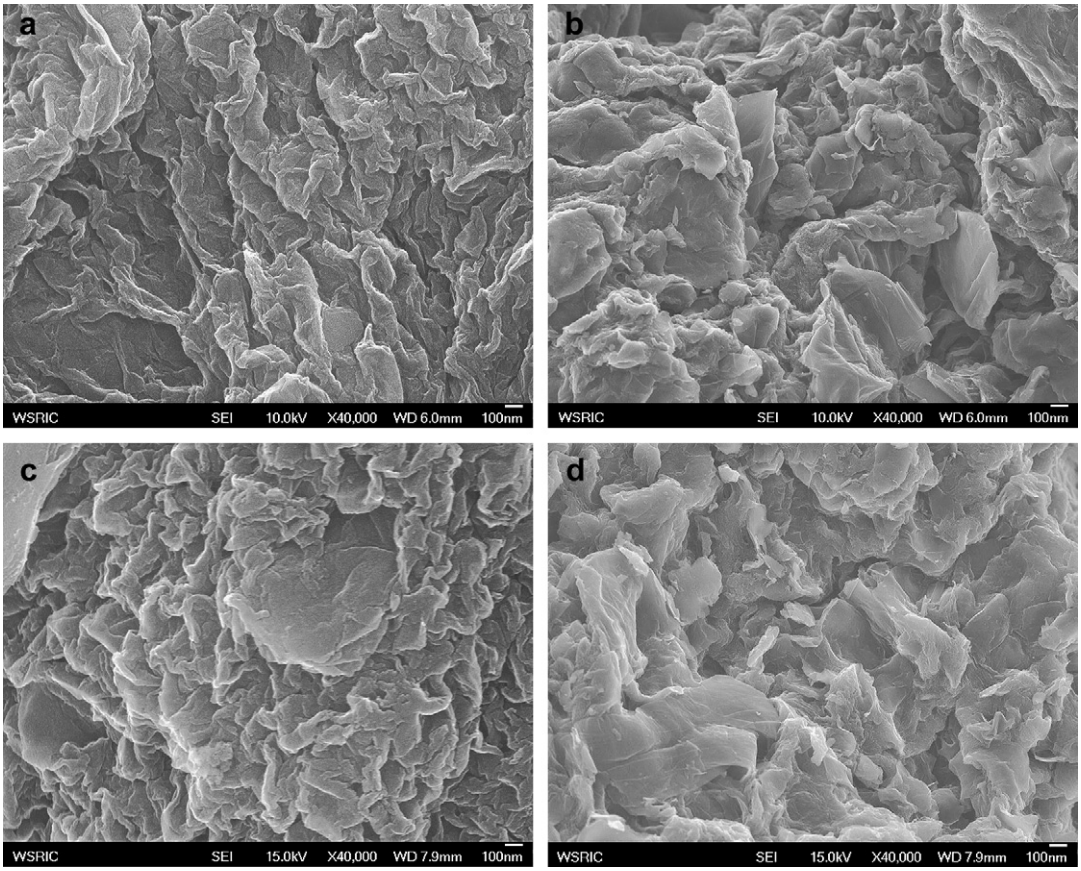

Fig. 7. (a–d): FESEM image of PPyGO1 composite (a); PPyGO2 composite (b); PPyGR1 composite (c); PPyGR2 composite (d).

I. Increased number of sp^2 domains formed during the in-situ reduction process, and
II. Presence of unrepaired defects that remained after the removal of large amounts of oxygen-containing functional groups [30,32].
III. Partially disordered crystal structure of in-situ formed graphene nanosheets.

Moreover, Paredes et al. [33] observed that the amorphous character of the carbon lattice in the GO which developed during the oxidation process, had converted to graphitic carbon lattice during reduction process and in the process increment in intensity ratio (I_D:I_G) was evident. Moreover, peaks at 932 and 1055 cm^{-1} in the Raman spectra of the PPy/GR composite has revealed the presence of doped PPy structures.

4.6. Measurements of electrical conductivity

The electrical conductivities (σ) of pure PPy, GR, PPy/GO, and PPy/GR composites are determined using a Keithley 2000 four-point probe resistivity measurement system. The average conductivities are summarized in Table 1. Pure PPy shows a conductivity of 0.19 S/cm, however, pure graphene shows a very high value of conductivity (47.60 S/cm). For PPyGO1, PPyGO2 and PPyGO3, the conductivities are 0.51, 1.41 and 1.64 S/cm respectively. Increase in magnitude of conductivity as compared to pure PPy may be attributed to the π–π stacking between the GO layers and PPy. After reduction, the conductivities of the reduced composites are significantly increased which is evident from Table 1. Substantial increment in conductivity is perhaps due to the high aspect ratio, large specific surface area of the in-situ formed graphene nanosheets in PPy matrix.

4.7. Thermogravimetric analysis

The Thermal stability of pure PPy, PPy/GO, and PPy/GR composites are shown in Fig. 6, with respective data are being summarized in Table 2. In the case of PPy/GO composites nearly a 7.9% weight loss has occurred at 100 °C, due likely to de-intercalation of water from the gallery space of the GO framework. The weight loss near 200 °C for the PPy/GO composites is presumably due to pyrolysis of the labile oxygen-containing functional groups. However, after removal of the oxygen functionality by hydrazine monohydrate, a considerable enhancement in thermal stability has been observed for PPy/GR composite at 200 °C. Only a mere 6.1 wt% weight loss has been observed for PPy/GR composites at 200 °C as compared to loss of 10.5 wt% for the PPy/GO composites which justified the improved thermal stability upon reduction of the PPy/GO composites. After 250 °C, major weight loss has occurred for all the concerned composites, perhaps due to decomposition of the PPy from the composite. Finally at 450 °C, weight loss for GO-based PPy composite is almost 23.4% more than that of GR-based composite. All the observation has revealed that GR-based PPy composite showed superior thermal stability than GO-based PPy composite.

4.8. Morphological observation

The morphology and structure of the PPy/GO, and PPy/GR composites are characterized using field emission transmission electron microscopy (FESEM) and the respective images are shown in Fig. 7(a–d). From FESEM study it is been observed that, PPyGO1 and PPyGO2 composites demonstrate a typically curved, layerlike structure and the GO sheets are surrounded by PPy (Fig. 7a and b). However, after reduction, the in-situ formed graphene sheets appeared as wrinkled form in PPy/GR composites (Fig. 7c and d).

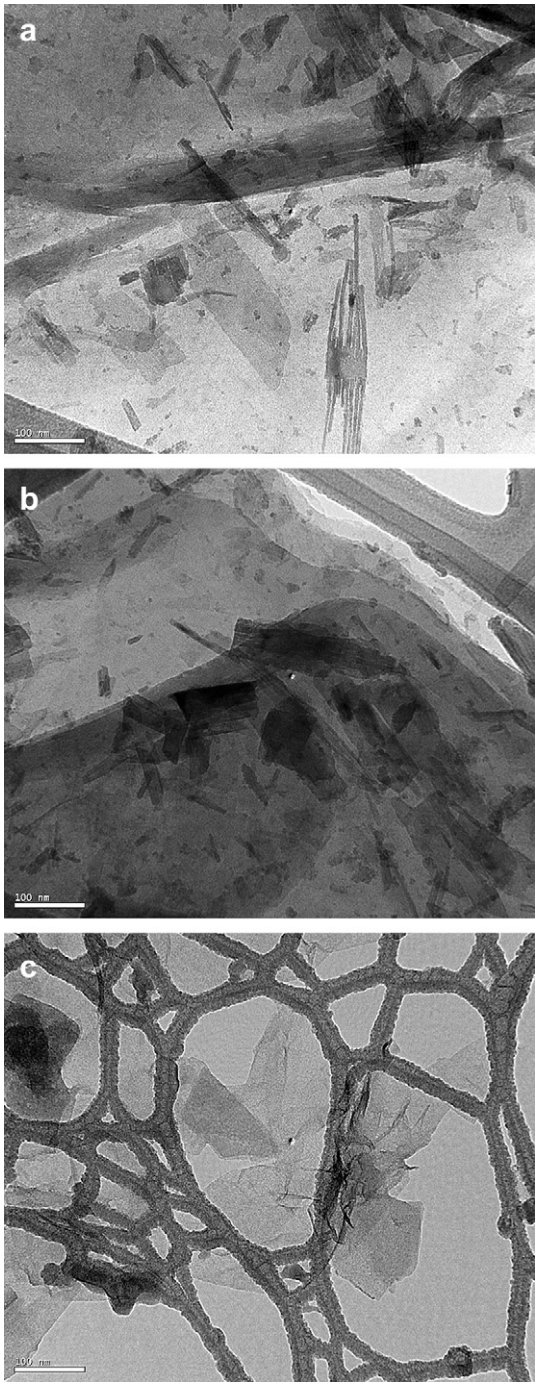

Fig. 8. (a–c): TEM image of PPy/GO composite (a); PPy/GR composite (b); pure GR (c).

The TEM images for PPy/GO, PPy/GR, and pure GR are shown in Fig. 8(a–c). Distribution of GO and GR in their respective composites is evident from Fig. 8a and b respectively.

5. Conclusions

PPy/GR composites were prepared by in-situ synthesis of GO and pyrrole monomer followed by chemical reduction using hydrazine monohydrate. The PPy/GR composites exhibited a high value of conductivity which may be attributed to the high aspect ratio and large specific surface area of the in-situ formed graphene nanosheets in PPy matrix. The XPS results demonstrated that the

C/O ratio for PPy/GR composites was 9.9, but for the PPy/GO composite it was 2.1, indicating the removal of oxygen functionality upon reduction. Formation of a graphene-like structure was further confirmed by the XRD study and FTIR spectroscopic analysis. As evident from Raman spectroscopy, intensity ratio was 1.17 for PPy/GR, suggesting the increased number of c-sp^2 domains which were formed during the reduction process. Distribution of graphene sheets throughout the PPy matrix was shown in TEM study. FESEM study revealed the appearance of a wrinkled and flaky morphology for the PPy/GR composites.

Acknowledgements

This study was supported by the National Space Lab (NSL) program (S1 08A01003210), the Human Resource Training Project for Regional Innovation, and World Class University (WCU) program (R31-20029) funded by the Ministry of Education, Science and Technology (MEST) and National Research Foundation (NRF) of Korea.

References

[1] Zhang HB, Zheng WG, Yan Q, Yang Y, Wang JW, Lu ZH, et al. Polymer 2010; 51(5):1191–6.
[2] Zhang YB, Tan YW, Stormer HL, Kim P. Nature 2005;438(7065):201–4.
[3] Stankovich S, Dikin DA, Dommett GHB, Kohlhaas KM, Zimney EJ, Stach EA, et al. Nature 2006;442(7100):282–6.
[4] Zhang YB, Small JP, Amori MES, Kim P. Phys Rev Lett 2005;94(17):176803.
[5] Berger C, Song Z, Li T, Li XB, Ogbazghi AY, Feng R, et al. J Phys Chem B 2004;108(52):19912–6.
[6] Balandin AA, Ghosh S, Bao WZ, Calizo I, Teweldebrhan D, Miao F, et al. Nano Lett 2008;8(3):902–7.
[7] Lee C, Wei XD, Kysar JW, Hone J. Science 2008;321(5887):385–8.
[8] Yang X, Li L, Shang S, Tao XM. Polymer 2010;51(15):3431–5.
[9] Heersche HB, Jarillo-Herrero P, Oostinga JB, Vandersypen LMK, Morpurgo AF. Nature 2007;446(7131):56–9.
[10] Wei T, Luo G, Fana Z, Zheng C, Yan J, Yao C, et al. Carbon 2009;47(9):2290–9.
[11] Chen G, Weng W, Wu D, Wu C. Eur Polym J 2003;39(12):2329–35.
[12] Liu N, Luo F, Wu H, Liu Y, Zhang C, Chen J. Adv Func Mater 2008;18 (10):1518–25.
[13] Nethravathi C, Rajamathi JT, Ravishankar N, Shivakumara C, Rajamathi M. Langmuir 2008;24(15):8240–4.
[14] Szabo T, Szeri A, Dekany I. Carbon 2005;43(1):87–94.
[15] Hu H, Wang X, Wang J, Wa L, Liu F, Zheng H, et al. Chem Phys Lett 2010;484 (4–6):247–53.
[16] Yu AP, Ramesh P, Itkis ME, Bekyarova E, Haddon RC. J Phys Chem Lett C 2007;111(21):7565–9.
[17] Liu Q, Liu Z, Zhang X, Yang L, Zhang N, Pan G, et al. Adv Funct Mater 2009; 19(6):894–904.
[18] Raghu AV, Lee YR, Jeong HM, Shin CM. Macromol Chem Phys 2008;209 (24):2487–93.
[19] Chen G, Wu D, Weng W, Wu C. Carbon 2003;41(3):619–21.
[20] Zhang K, Zhang LL, Zhao XS, Wu J. Chem Mater 2010;22(4):1392–401.
[21] Wu TM, Chang HL, Lin YW. Compos Sci Tech 2009;69(5):639–44.
[22] Wu TM, Lin SH. J Polym Sci Part A Polym Chem 2006;44(21):6449–57.
[23] Yan J, Wei T, Shao B, Fan Z, Qian W, Zhang M, et al. Carbon 2010; 48(2):487–93.
[24] Gu Z, Zhang L, Li C. J Macromol Res;Part B 2009;48(6):1093–102.
[25] Jeong HK, Noh HJ, Kim JY, Jin MH, Park CY, Lee YH. J Explor Front Phys 2008; 82(6):67004.
[26] Bissessur R, Liu PKY, Scully SF. Synth Met 2006;156(16–17):1023–7.
[27] Nakajima T, Mabuchi A, Hagwara R. Carbon 1988;26(3):357–61.
[28] Gao J, Liu F, Liu Y, Ma N, Wang Z, Zhang X. Chem Mater 2010;22(7):2213–8.
[29] Fan Z, Wang K, Wei T, Yan J, Song L, Shao B. Carbon 2010;48(5):1686–9.
[30] Stankovich S, Dikin DA, Piner RD, Kohlhaas KA, Kleinhammes A, Jia Y, et al. Carbon 2007;45(7):1558–65.
[31] Tuinstra F, Koenig JL. J Chem Phys 1970;53(3):1126–30.
[32] Zhou Y, Bao QL, Tang LAL, Zhong YL, Loh KP. Chem Mater 2009; 21(13):2950–6.
[33] Paredes JI, Villar-Rodil S, Solis-Fernandez P, Martinez-Alonso A, Tascon JMD. Langmuir 2009;25(10):5957–68.